**Chapter 1**

# NEW WAYS OF ANALYSING CHEMICAL BONDING

Dieter Cremer
Lehrstuhl für Theoretische Chemie
Universität Köln

**Abstract:** An analysis of the total electron density distribution $\rho(\mathbf{r})$ with the aid of its gradient vector field $\nabla\rho(\mathbf{r})$ and its Laplace distribution $\nabla^2\rho(\mathbf{r})$ leads to a physically meaningful definition of an atom in a molecule and chemical bonding. Utilizing these definitions one can determine bond order, $\pi$ character, bond polarity, and bent bond character of covalent bonds from the properties of $\rho(\mathbf{r})$ in the bonding region. Investigation of the Laplacian of $\rho(\mathbf{r})$ provides insight into the electronic structure of atoms and molecules and allows useful predictions with regard to their chemical reactivity.

## Introduction

Valuable information about chemical bonding has been and is obtained from an analysis of the electron density distribution $\rho(\mathbf{r})$ /1-3/. Although the latter is a molecular property that can be obtained from X-ray and neutron diffraction experiments, it is seldom analysed directly. Instead, $\rho(\mathbf{r})$ is used to construct

difference or deformation electron densities $\Delta\rho(\mathbf{r})$ /4/:

$$\Delta\rho(\mathbf{r}) = \rho(\text{molecule}) - \rho(\text{promolecule}) \qquad . \qquad (1)$$

The density of the promolecule is obtained by a superposition of atomic densities where the atoms are considered to be a) in their ground state, b) neutral, c) noninteracting, and d) located in positions which they adopt in the molecule. In the case of atoms with spatially degenerate ground states such as the P states of C, O, and F the atomic densities are spherically averaged/4/.

The analysis of the difference density offers a number of advantages, in particular for the crystallographer. In addition, it leads to a seemingly simple description of chemical bonding: Accumulation of electron density in the bonding area, indicated by a positive difference (deformation) density $(\Delta\rho > 0)$, acts as an electrostatic glue that keeps the atomic nuclei together and leads to chemical bonding.

Although the description of chemical bonding with the aid of the difference (deformation) electron density seems to be simple and very appealing, it suffers from serious drawbacks. These become obvious when investigating covalent bonds between electronegative atoms. For example, Savariault and Lehmann/5/ obtained a negative deformation electron density in the OO bonding region of $H_2O_2$ when investigating the molecule by X-ray and neutron diffraction. Negative or very small difference (deformation) densities have also been found in certain CN, CO, and CF bonds of various organic molecules by Dunitz and co-workers/6/. These bonds have been considered as bonds "without bonding electron density", a description that is largely misleading. A negative difference (deformation) density is simply a result of the choice of the reference density $\rho(\text{promolecule})$ in equation 1/7,8/. A promolecular reference density can be defined in many ways. Instead of using spherically averaged atomic

densities when constructing ρ(promolecule), one can use "oriented" atomic densities /8/. Also one can consider the electron density of those states to which the molecule will actually dissociate/9/. It is hardly possible to say which choice is better. The derivation of an unique and physically meaningful difference (deformation) electron density is a problem that cannot be solved since the choice of the promolecular reference density always implies some arbitrariness/10/.

As a consequence, there is no way of getting to a consistent description of chemical bonds by means of experimentally or theoretically obtained difference densities. A consistent description can only be achieved if one analyses the total electron density distribution $\rho(r)$ and refrains from using artificially derived reference densities.

## Analysis of the Electron Density Distribution

In Figure 1 the calculated electron density distribution $\rho(r)$ of benzene is shown with regard to the molecular plane in the form of a perspective drawing. At the positions of the nuclei, $\rho(r)$ attains maximal values. In the off-nucleus direction, $\rho(r)$ decreases exponentially and approaches zero for large $r$. This will be different if one considers the region between two nuclei belonging to bonded atoms, e.g. a C,H bond region (Figure 1). In this region $\rho(r)$ adopts fairly large values. *The nuclei are connected by a path of maximum electron density (MED path).* Any lateral displacement from the MED path leads to a decrease in $\rho(r)$. The position $r_B$ of the minimum of $\rho(r)$ along the MED path is a point which can be used to characterize the density distribution in the internuclear region. The position $r_B$ corresponds to a maximum of $\rho(r)$ in the directions perpendicular to the MED path, i.e. it is a first order saddle point of $\rho(r)$ in three dimensions.

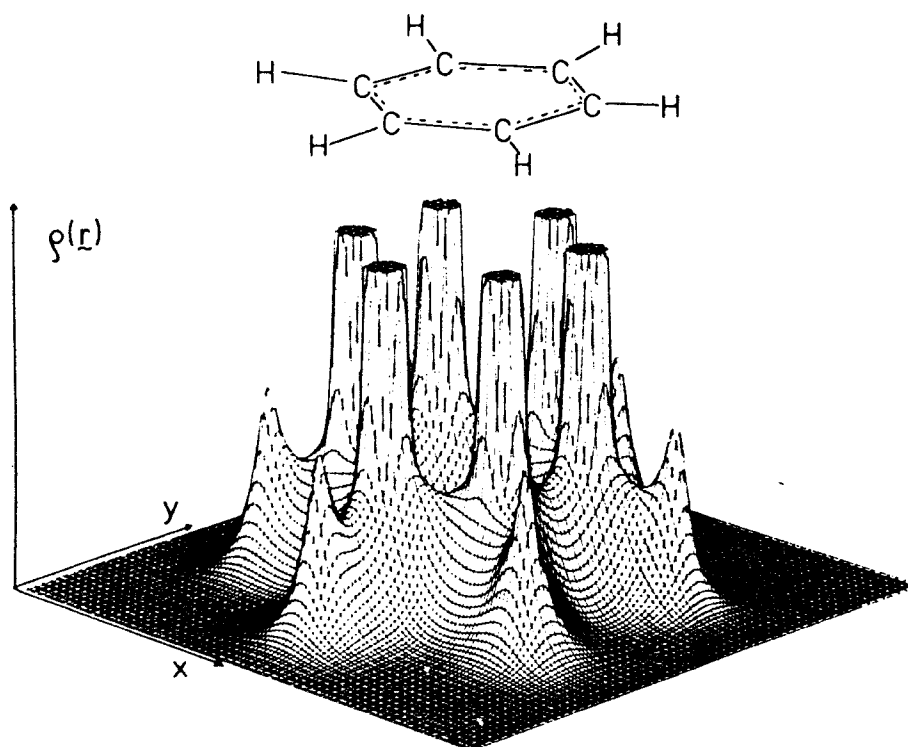Fig. 1: Perspective drawing of the electron density distribution $\rho(r)$ of benzene shown with regard to the plane of the atomic nuclei (HF/6-31G* calculations). In this and the following figures the function value has been cut off above a predetermined value in order to improve the representation.

The saddle point $r_B$ is fully characterized by the first and second derivatives of $\rho(r)$ with regard to $r$: The gradient of $\rho(r)$, $\nabla\rho(r)$, vanishes at $r_B$ and two of the three eigenvalues (curvatures) $\lambda_i$ (i = 1,2,3) of the Hessian matrix of $\rho(r)$, i.e. the matrix of second derivatives, are negative. The curvatures $\lambda_1$ and $\lambda_2$ perpendicular to the MED path are negative while the curvature $\lambda_3$ along the MED path is positive due to the minimum of $\rho(r)$ in this direction.

If one analyses the gradient of $\rho(\mathbf{r})$ not only at the point $\mathbf{r}_B$ but also at other points in molecular space, then the gradient vector field of $\rho(\mathbf{r})$ will be obtained. The gradient vector $\nabla\rho(\mathbf{r})$ always points into the direction of a maximum increase in $\rho(\mathbf{r})$. Thus, each such vector is directed toward some neighboring point. By calculating $\nabla\rho(\mathbf{r})$ at a continuous succession of points, a trajectory of $\nabla\rho(\mathbf{r})$, the path traced out by the gradient vector of $\rho(\mathbf{r})$, is obtained

In Figure 2, $\rho(\mathbf{r})$ and $\nabla\rho(\mathbf{r})$ of the HCN molecule are shown, both with regard to a reference plane containing the nuclei. One can distinguish three types of trajectories in the gradient vector field:

First, there are those trajectories which terminate at one of the nuclei. The space traversed by all trajectories terminating at one and the same nucleus is called the *basin of the nucleus. An atom in a molecule can be defined as the union of the nucleus and its associated basin*, a definition which was suggested by Bader and co-workers/11/.

If two atoms defined in this way are bonded, their basins will be adjoined and there will be a surface of demarkation between them. Such an interatomic surface is made up of the second class of trajectories, those that terminate at a saddle point $\mathbf{r}_B$ rather than at a nucleus. In case of HCN (Figure 2b), the three atomic basins are separated by two interatomic surfaces, of which one can only see the traces g in the two-dimensional representation.

The third class of trajectories comprises those gradient vector paths s which spring at one of the saddle points $\mathbf{r}_B$ and terminate at a nucleus. Just two of these trajectories mark the MED path linking two nuclei (see Figure 2b).
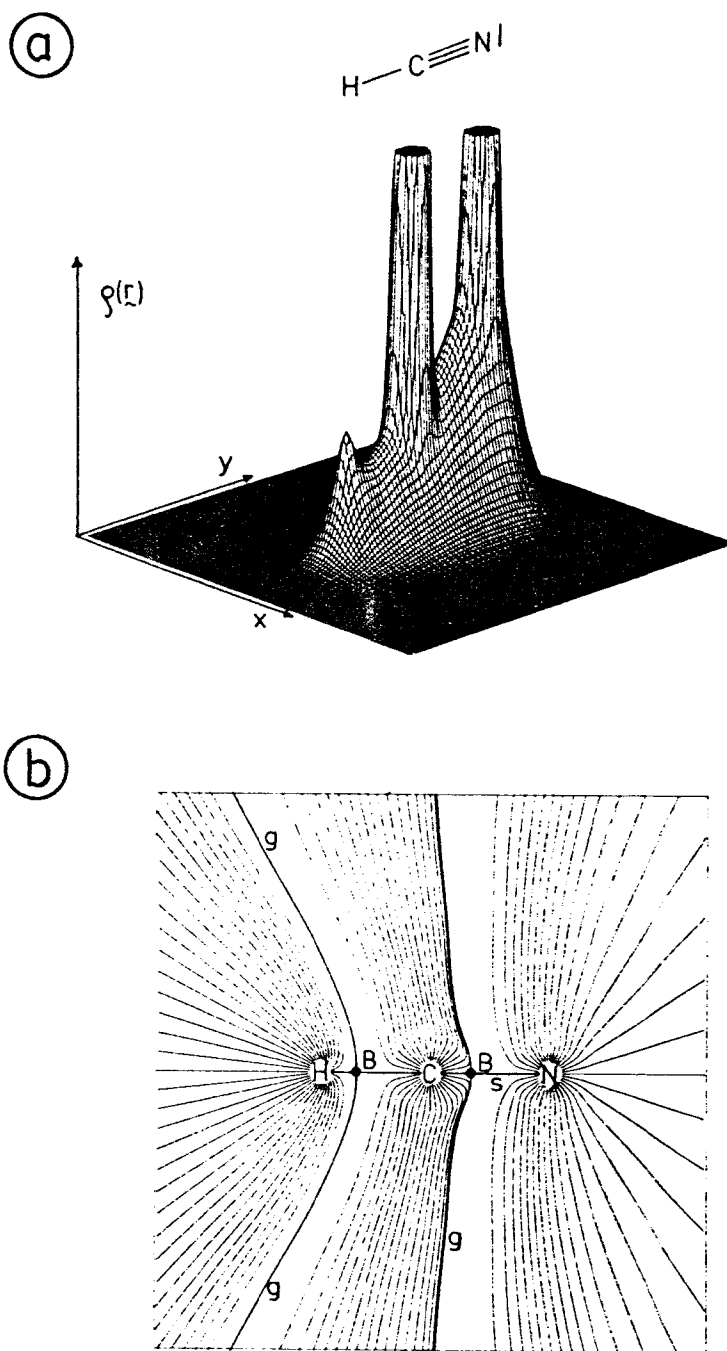
Figure 2. a) Perspective drawing of the electron density distribution $\rho(\mathbf{r})$ of HCN shown with regard to a plane that contains the nuclei. b) Gradient vector field $\nabla\rho(\mathbf{r})$ of HCN. B denotes the saddle point $\mathbf{r}_B$, s the MED path, and g the trace of the interatomic surface in the reference plane (HF/6-31G* calculation).

By analysing $\rho(\mathbf{r})$ via its gradient vector field one can easily determine atomic basins, interatomic surfaces, and MED paths linking the atomic nuclei in a molecule.

## Definition of a Chemical Bond

Analysis of the electron density distribution $\rho(\mathbf{r})$ of numerous molecules /12-14/ has revealed that there exists a one to one relation between MED paths, saddle points $\mathbf{r}_B$, and interatomic surfaces on the one side and chemical bonds on the other side.

This relation is the basis for a definition of a chemical bond/13,14/:

*Two atoms will be bonded if and only if there exists a MED path linking them (necessary condition).*

One can also formulate a sufficient condition of chemical bonding by analyzing the local energy density $H(\mathbf{r})$ in the bonding area/13,14/:

$$H(\mathbf{r}) = G(\mathbf{r}) + V(\mathbf{r}) \qquad , \qquad (2)$$

where $G(\mathbf{r})$ is a local kinetic energy density and $V(\mathbf{r})$ is the local potential energy density /15/. If $H(\mathbf{r})$ is negative, then the local potential energy density $V(\mathbf{r})$ will dominate and an accumulation of electronic charge in the internuclear region will be stabilizing. In this case we speak of a *covalent bond*. The MED path is an image of the covalent bond and, therefore, it is called the *bond path*. For the same reason, $\mathbf{r}_B$ is termed *bond critical point*/16/.

If $H(\mathbf{r})$ is zero or positive in the internuclear region, then there will be closed shell interactions between the atoms in question, typical of ionic bonding, hydrogen bonding or van der Waals interactions/14/.

On the basis of these definitions one can describe chemical bonding in molecules with the aid of the properties of $\rho(\mathbf{r})$. One starts by searching for the bond paths and their associated bond critical points $\mathbf{r}_B$ in the molecular electron density distribution. If all bond paths are found, then the properties of $\rho(\mathbf{r})$ along the bond paths will be used to characterize the chemical bonds. For example, the value of $\rho(\mathbf{r})$ at the bond critical point $\mathbf{r}_B$ can be used to determine a bond order, the anisotropy of $\rho(\mathbf{r}_B) = \rho_B$ can be related to the $\pi$ character of a bond, the position of the bond critical point $\mathbf{r}_B$ is a measure of the bond polarity, and the curvature of the bond path reveals the bent-bond character of a bond /14/.

## Description of Covalent Bonds

In Figure 3, a correlation between $\rho_B$, the calculated electron density at the bond critical point $\mathbf{r}_B$, and the CC bond distance R, both calculated for a variety of hydrocarbons, is shown. A linear relationship is obtained which holds for both single, double, triple, and aromatic CC bonds, for strained as well as unstrained CC bonds /12,14/. On the basis of this relationship, a *bond order* n(CC) has been defined /12/. By assigning Lewis bond orders of 1, 2, and 3 to ethane, ethylene, and acetylene the logarithmic relationship between n and $\mathbf{r}_B$ given in Figure 4 is obtained. Utilizing this equation, bond orders close to 1.5 are calculated for Hückel aromatic systems such as benzene, the tropylium cation or the cyclopentadienyl anion /12/. This is in agreement with the idea of $\pi$ delocalization in these compounds.

One can also define bond orders for molecules containing nitrogen or oxygen atoms /14/. In this way, one gets a particularly simple tool of describing bonding in molecules, a tool, which is familiar to the experimentalist and which does not suffer from the ambiguities of an analysis of chemical bonding in terms of molecular orbitals /17/.
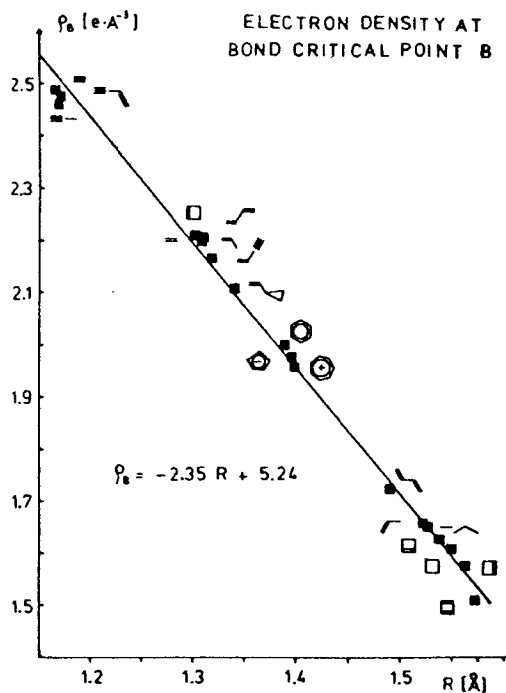
Figure 3. Relationship between $\rho_B$, the electron density at $r_B$, and the bond length R(CC) (HF/STO-3G calculations /12/).
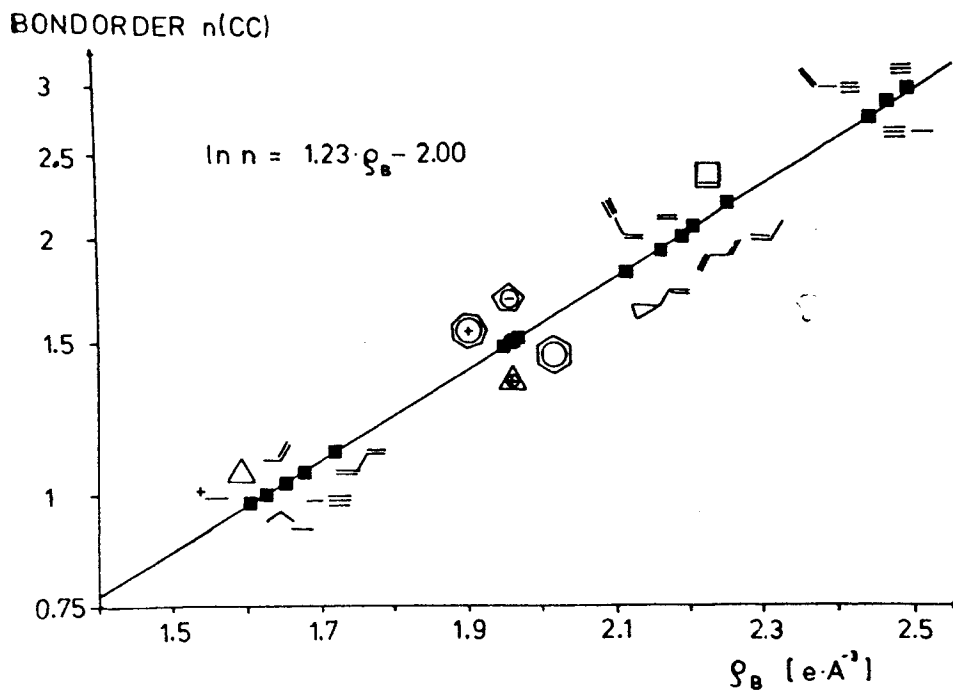


Figure 4. Definition of a bond order n for CC bonds (HF/STO-3G calculations /12/).

Another insight into the nature of a covalent bond is provided by analysing the anisotropy of the electron density distribution $\rho(r)$ at the bond critical point $r_B$. In Figure 5, contour line diagrams of $\rho(r)$ of ethane and ethylene are schematically shown with regard to the plane which is perpendicular to the CC bond and which contains $r_B$.



$$\epsilon = \frac{\lambda_1}{\lambda_2} - 1 = 0 \qquad\qquad \epsilon = \frac{\lambda_1}{\lambda_2} - 1 = 0.74$$
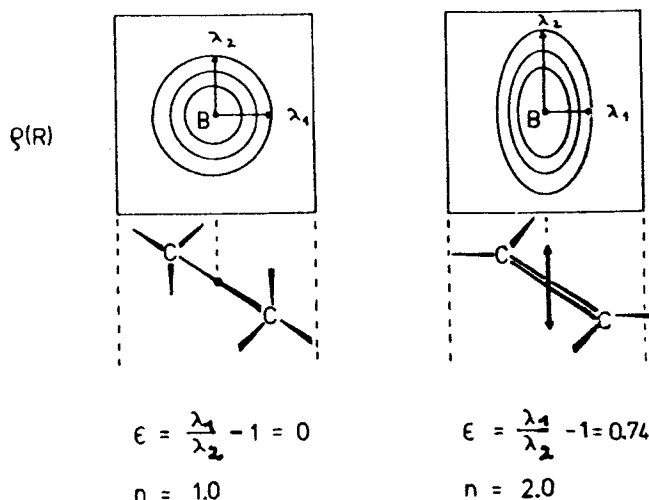
$$n = 1.0 \qquad\qquad\qquad n = 2.0$$

Figure 5. Qualitative illustration of the electron density distribution at the CC bond critical point $r_B$ of ethane and ethylene. The directions of steep $(\lambda_1)$ and soft curvature $(\lambda_2)$ are indicated. The latter is taken as the "direction" of the bond ellipticity $\epsilon$ and is indicated by the double-head arrow (HF/STO-3G calculations /12/).

In the case of the single bond, the contour lines are concentric with regard to $r_B$ according to an isotropical distribution of the electron density at the CC single bond. For the CC double bond, however, the contour lines of $\rho(r)$ are elliptic. The electron density extends more into space in the direction of the $\pi$ orbitals than perpendicular to them. This is reflected by the eigenvalues $\lambda_1$ and $\lambda_2$ of the Hessian matrix, the curvatures of $\rho(r)$ perpendicular to the

bond axis. The ratio $\lambda_1$ to $\lambda_2$ has been used to define the bond ellipticity $\varepsilon$ /12/:

$$\varepsilon = \lambda_1 / \lambda_2 - 1 \qquad , \qquad (3)$$

which is a measure of the anisotropy of $\rho(\mathbf{r})$ at $\mathbf{r}_B$. A direction has been assigned to $\varepsilon$, namely the direction of the soft curvature measured by $\lambda_2$. This direction is called the major axis of $\varepsilon$ /12/. It is indicated by the double-headed arrow in Figure 5.

Although a distinction between $\sigma$ and $\pi$ electrons is no longer appropriate when analysing $\rho(\mathbf{r})$, it is nevertheless appealing to relate the bond ellipticity $\varepsilon$ to the $\pi$ *character* of a double bond /12,14/. Calculated bond orders n and bond ellipticities $\varepsilon$ are shown in Figure 6.

For planar $\pi$ systems the major axis of $\varepsilon$ is always perpendicular to the molecular plane, i.e. all major axes are parallel. One can say that the bond ellipticities overlap completely. In the case of benzene the values of $\varepsilon$ are all equal indicating that the $\pi$ electrons are fully delocalized. For *trans* 1,3-butadiene and cyclobutadiene, the bond ellipticities of the double bonds propagate to some extent into the formal single bonds revealing that the latter possess partial $\pi$ character. The degree of $\pi$ conjugation can be quantitatively assessed by the calculated n and $\varepsilon$ values /12,14/. In the same way, the extent of hyperconjugation in compounds such as propene or the ethyl cation is reflected by the calculated values of n and $\varepsilon$ (Figure 6).

Another interesting information about the nature of a chemical bond is provided by the position of the bond critical point. The position $\mathbf{r}_B$ depends on the electronegativities of the atoms connected and, therefore, provides a measure of the *bond polarity* /14/. This is illustrated in Figure 7 for a number of
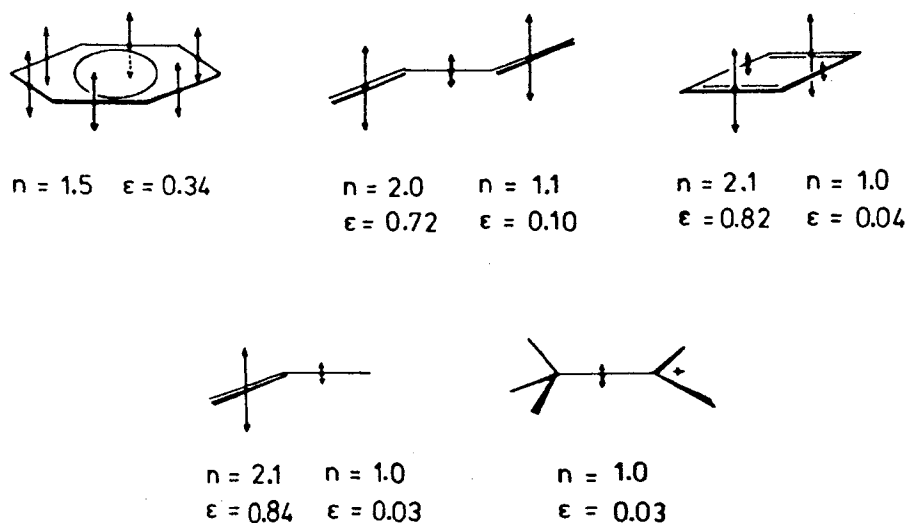
n = 1.5   ε = 0.34       n = 2.0    n = 1.1       n = 2.1    n = 1.0
                         ε = 0.72   ε = 0.10      ε = 0.82   ε = 0.04

n = 2.1   n = 1.0        n = 1.0
ε = 0.84  ε = 0.03       ε = 0.03

Figure 6. Calculated bond orders n(CC) and bond ellipticities ε(CC) of some hydrocarbons (HF/STO-3G calculations).
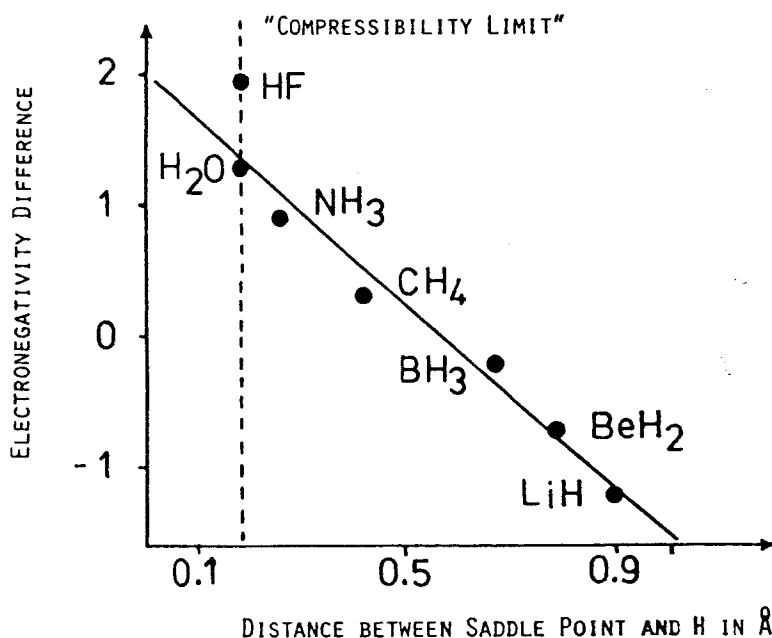


Figure 7. Correlation of the electronegativity difference $\Delta\chi = \chi(A) - \chi(H)$ with the distance $r_B, r_H$ for $AH_n$ molecules (HF/6-31G** calculations /10,14/).

hydrides $AH_n$. The bond critical point $r_B$ is always closer to the more electropositive atom, e.g. closer to Li than H in LiH. The basin of the former atom is smaller since it has lost part of its negative charge to the more electronegative atom, namely H. When the electronegativity of A increases, $r_B$ of the bond AH moves toward the H atom (Figure 7). For $H_2O$ a compressibility limit is reached which cannot be exceeded /14/. Taking this into account, one directly gets information about the bond polarity when determining the bond critical point $r_B$.

A feature of the chemical bond which is discussed in many textbooks, but which is difficult to describe on a quantitative basis, is its bent bond character. The analysis of $\rho(r)$ along the lines described above immediately leads to a quantitative determination of the bending of a bond. In many cases, in particular in the case of strained molecules, the bond path does not coincide with the internuclear connection line. Such a situation is shown schematically for cyclopropane in Figure 8. The dashed lines indicate the CC bond paths which are curved outwardly. The point $r_B$ is shifted by
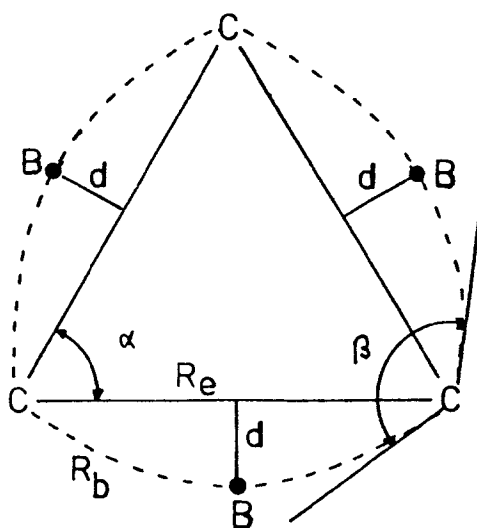


Figure 8. Schematic representation of the bending of the CC bond paths (dashed lines) in cyclopropane. For the definition of the parameters, see text.

a distance $d$ from the internuclear connection line. As a consequence, the bond path length $R_b$ is longer than the internuclear distance $R_e$. For example, the length of the CC bond paths in cyclopropane is 1.52 Å rather than 1.50 Å, the experimentally determined value of $R_e$ /18/.

Similarly, the interpath angle $\beta$, i.e. the angle between the CC bond paths (Figure 8), can be considerably larger than the geometrical angle $\alpha$. In the case of cyclopropane it is 79° rather than 60° /18/. The former value is physically meaningful and can be used to determine the strain energy of cyclopropane /19/.

## The Laplacian of the Electron Density Distribution

An analysis of $\rho(r)$ leads to useful information about bond order (strength), $\pi$ character, bond polarity, and bent bond character. Additional information can be gained by analysing not only $\rho(r)$ and $\nabla\rho(r)$ but also $\nabla^2\rho(r)$, the Laplacian of the electron density distribution. The Laplacian of a scalar function f indicates where this function concentrates ($\nabla^2 f < 0$) and where it is depleted ($\nabla^2 f > 0$) /20/, i.e. in the case of $\rho(r)$ the *Laplace concentration*, $-\nabla^2\rho(r)$, reveals where the electrons lump together in the molecule /21/.

In Figure 9, this is illustrated for the N atom in its $^4S$ ground state. Contrary to $\rho(r)$, which is characterized by a maximal value at the position of the nucleus and an exponential decay in the off-nucleus direction, the Laplace concentration of $N(^4S)$ reveals an interesting pattern. Close to the nucleus there is a peak of high electron concentration, which is surrounded by a sphere of charge depletion. Further away from the nucleus, a second sphere with concentration of negative charge is found (Figure 9). It is appealing to assign the inner sphere of charge
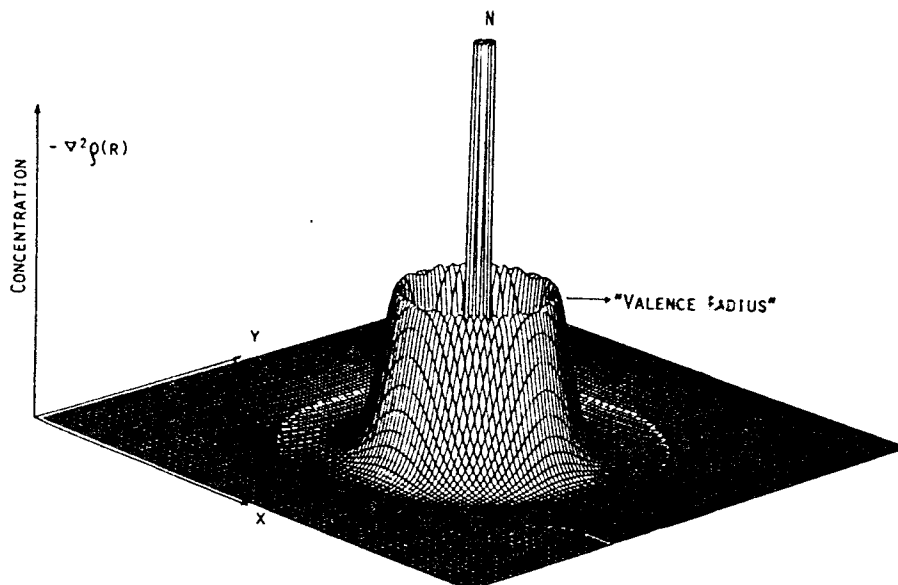
Figure 9. Perspective drawing of the Laplace concentration, $-\nabla^2\rho(\mathbf{r})$, of the the N atom in its $^4$S ground state.
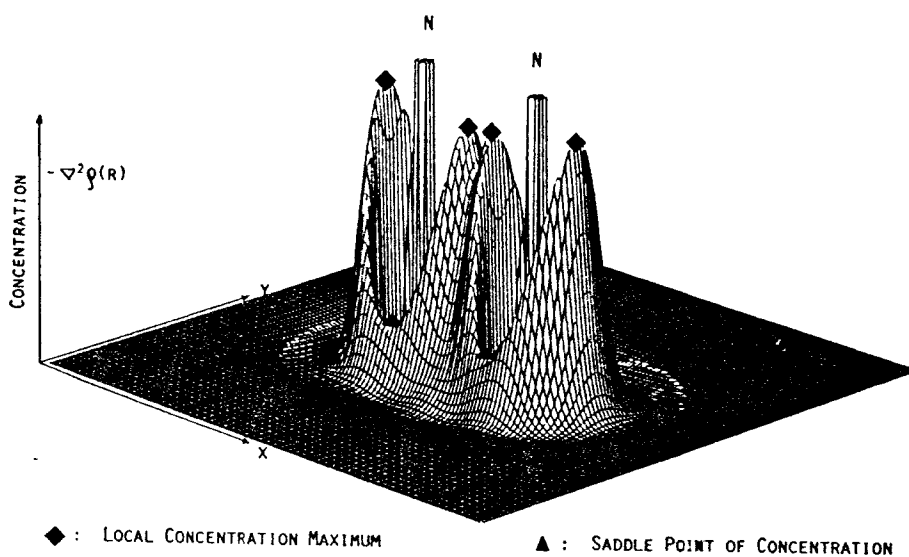


Figure 10. Perspective drawing of the Laplace concentration, $-\nabla^2\rho(\mathbf{r})$, of the $N_2$ molecule (HF/6-31G* calculation).

to the valence electrons. Accordingly, one can speak of an inner shell and a valence shell of the Laplacian of $\rho(\mathbf{r})$: *The distribution $-\nabla^2\rho(\mathbf{r})$ reflects the shell structure of the atom* /21/.

If two atoms bind, the shell structure of the Laplacian of $\rho(\mathbf{r})$ is deformed in a characteristic way as is shown in Figure 10 for the case of the $N_2$ molecule. Electrons lump together in the bonding and in the nonbonding regions. Again, it is very appealing to assign regions with large concentrations of $\rho(\mathbf{r})$ to electron bond and electron lone pairs. The holes in the valence concentrations, which develop when two N atoms form the $N_2$ molecule, may be considered as positions prone to a nucleophilic attack.

This is shown more clearly in Figure 11 which depicts a perspective drawing of the calculated Laplace concentration $-\nabla^2\rho(\mathbf{r})$ of HCN. One can recognize the 1s concentrations of H, C, and N atom, then the electron bond pair (bp) concentrations in the HC and CN bonding regions and, finally, the electron lone pair (lp) concentration at the N atom. Clearly, an electrophile will preferentially attack at the lone pair side of the N atom. There are large holes in the valence sphere of the C atom of HCN, in which the lone pair concentration of a nucleophile would fit. It is reasonable to predict that a nucleophile will preferentially attack at the carbon atom of HCN /22/. Hence, the Laplace concentration provides useful information about the electronic structure of a molecule and allows predictions with regard to its reactive behavior.

One could argue that all the information extracted either from $\rho(\mathbf{r})$ or $\nabla^2\rho(\mathbf{r})$ could also be obtained by analysing the molecular orbitals. Why should one invest additional effort in calculating and analysing the electron density distribution? An answer to this question can be given in three parts:
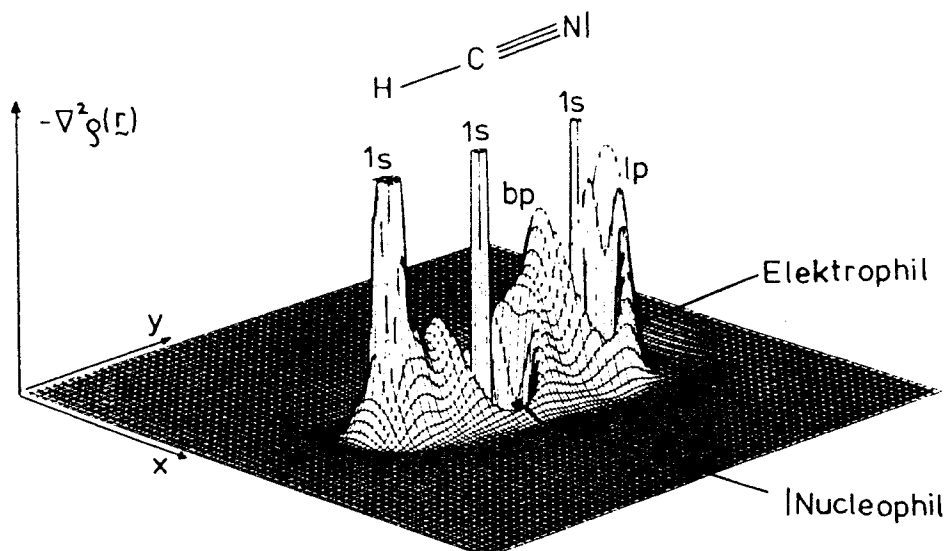
Figure 11. Perspective drawing of the Laplace concentration, $-\nabla^2\rho(r)$, of HCN (HF/6-31G* calculation /22/). Charge concentrations assigned to the 1s electrons, bonding electron pairs (bp), and the electron lone pair (lp) of N are indicated. Probable positions of electrophilic or nucleophilic attack are also given.

First of all, it is advantageous to have two rather than one tool for investigating the electronic structure of a molecule. One can check whether the analysis of $\rho(r)$ and the analysis of the molecular orbitals lead to identical, complementary or contradictory descriptions of the molecule and its properties. Calculation of $\rho(r)$ and $-\nabla^2\rho(r)$ is not expensive. It is done in a time only marginally longer than that needed for a Mulliken population analysis /10,12/.

Secondly, the analysis of $\rho(r)$ and $-\nabla^2\rho(r)$ is carried out on a sound quantum mechanical basis. It has been shown by Bader and co-workers/11/ that all the quantum mechanics valid for the total molecular space is also valid for the atomic subspaces defined with the aid of the gradient vector field of $\rho(r)$, $\nabla\rho(r)$. This has to do with the fact that the total electron density distribution is an observable while the molecular

orbitals are nonobservable. Hence, the analysis of $\rho(\mathbf{r})$ should be more satisfying in the long run.

Finally, one has to stress that the analysis of $\rho(\mathbf{r})$ leads to answers to pending chemical problems. These answers are difficult to obtain by an investigation of the molecular orbitals. This has been demonstrated when investigating aromatic /23/ and homoaromatic compounds /24/, the electronic structure of three-membered rings and $\pi$ complexes /18/, the bonding in C,Be compounds /25/ and dications /26/, and the strain in small rings /19/. Also, the analysis of the electron density distribution has played an important role when rationalizing the calculational predictions of helium organic compounds /27/.

# References

1. *Electron Distributions and the Chemical Bond,* P. Coppens and M.B. Hall, (Eds.), Plenum Press, New York, 1982.
2. *Electron and Magnetization Densities in Molecules and Crystals,* P. Becker, (Ed.), Plenum Press, New York, 1978.
3. M. Breitenstein, H. Dannöhl, H. Meyer, A. Schweig, R. Seeger, U. Seeger, and W. Zittlau, *Int. Rev. Phys. Chem.* **3** (1983) 335.
4. P. Coppens and E.D. Stevens, *Adv. Quantum Chem.* **10** (1977) 1; P. Coppens, *Angew. Chem.* **89** (1977) 33.
5. J.M. Savariault and M.S. Lehmann, *J. Amer. Chem. Soc.* **102** (1980) 1298.
6. J.D. Dunitz and P. Seiler, *J. Amer. Chem. Soc.* **105** (1983) 7056; J.D. Dunitz, W.B. Schweizer, and P. Seiler, *Helv. Chim. Acta* **66** (1983) 123; P. Chakrabarti, P. Seiler, and J.D. Dunitz, *J. Amer. Chem. Soc.* **103** (1981) 7378.
7. K. Angermund, K.H. Claus, R. Goddard, and C. Krüger, *Angew. Chem.* **97** (1985) 241.

8. W.H.E. Schwarz, P. Valtazanos, and K. Ruedenberg, *Theor. Chim. Acta* **68** (1985) 471.

9. R.F.W. Bader in *The Force Concept in Chemistry*, B.M. Deb (Ed.), Van Nostrand Reinhold Company, New York, 1981, p. 39.

10. E. Kraka, Ph. D. Thesis, Universität Köln, 1984.

11. R.F.W. Bader, T.T. Nguyen-Dang, and Y. Tal, *Rep. Prog. Phys.* **44** (1981) 893; R.F.W. Bader and T.T. Nguyen-Dang, *Adv. Quantum Chem.* **14** (1981) 63.

12. R.F.W. Bader, T.S. Slee, D. Cremer, and E. Kraka, *J. Amer. Chem. Soc.* **105** (1983) 5061.

13. D. Cremer and E. Kraka, *Angew. Chem.* **96** (1984) 612; *Int. Ed. Engl.* **23** (1984) 627.

14. D. Cremer and E. Kraka, *Croat. Chem. Acta* **57** (1984) 1259.

15. R.F.W. Bader, *J. Chem. Phys.* **73** (1980) 2871. $G(r)$ is always positive while $V(r)$ is always negative. When integrated over total molecular space, they yield the kinetic and potential enrgy of a molecule: $E = \int H(r) \, dr = \int G(r) \, dr + \int V(r) \, dr$.

16. Note that Bader /11/ uses these terms differently by calling all MED paths, also those between closed shell systems, bond paths. This, however, is contrary to general chemical understanding.

17. Of course, the analysis of $\rho(r)$ at a single point $r_B$ rather than in the whole bonding region is a simplification. Also the bond order defined in such a way depends on the theoretical method used. For a detailed discussion of these points see Refs. 12 and 14.

18. D. Cremer and E. Kraka, *J. Amer. Chem. Soc.* **107** (1985) 3800, 3811.

19. D. Cremer and J. Gauss, *J. Amer. Chem. Soc.* **108** (1986) 7467.

20. P.M. Morse, H. Feshbach, *Methods of Theoretical Physics*, Vol. **1**, McGraw-Hill, New York 1953, p. 6.

21. R.F.W. Bader and H. Essen, *J. Chem. Phys.* **80** (1984) 1943.

22. D. Cremer, *Jahrbuch Akad. Wiss. Göttingen* (1984), 19.

23. D. Cremer and T. Schmidt, *J. Org. Chem.* **50** (1985) 2684.

**24.** D. Cremer, E. Kraka, T.S. Slee, R.F.W. Bader, C.D.H. Lau, and T.T. Nguyen-Dang, *J. Amer. Chem. Soc.* **105** (1983) 5069.

**25.** W. Koch, G. Frenking, J. Gauss, D. Cremer, A. Sawaryn, and P. v. R. Schleyer, *J. Amer. Chem. Soc.* **108** (1986) 5732.

**26.** W. Koch, G. Frenking, J. Gauss, and D. Cremer, *J. Amer. Chem. Soc.* **108** (1986) 5808.

**27.** W. Koch, G. Frenking, J. Gauss, D. Cremer, and J.R. Collins, *J. Amer. Chem. Soc.*, in press.